

where

$$\begin{pmatrix} \mathbf{K}_1(t_f) \\ \mathbf{K}_2(t_f) \end{pmatrix} = 0 \quad (3.11)$$

For the case when the acceleration and "jerk" terms are taken into account, the closed-form solutions for \mathbf{K}_1 and \mathbf{K}_2 are

$$\mathbf{K}_1 = \frac{(t_f - t)^3}{1/C_1 + \frac{1}{3}(t_f - t)^3} \left[\frac{\mathbf{a}_T}{2} + \frac{\dot{\mathbf{a}}_T}{6} (t_f - t) - \frac{(\mathbf{T} - \mathbf{D})}{2} - \frac{(\dot{\mathbf{T}} - \dot{\mathbf{D}})}{6} (t_f - t) \right] \quad (3.12)$$

$$\mathbf{K}_2 = \frac{(t_f - t)^2}{1/C_1 + \frac{1}{3}(t_f - t)^3} \left[\frac{\mathbf{a}_T}{2} + \frac{\dot{\mathbf{a}}_T}{6} (t_f - t) - \frac{(\mathbf{T} - \mathbf{D})}{2} - \frac{(\dot{\mathbf{T}} - \dot{\mathbf{D}})}{6} (t_f - t) \right] \quad (3.13)$$

Thus, Eq. (3.8) leads to the desired optimal control law, finite for all flight times:

$$\mathbf{a}_M = \frac{(t_f - t)}{1/C_1 + \frac{1}{3}(t_f - t)^3} \left[\mathbf{x} + \mathbf{v}(t_f - t) + \frac{\mathbf{a}_T}{2} (t_f - t)^2 + \frac{\dot{\mathbf{a}}_T}{6} (t_f - t)^3 - \frac{(\mathbf{T} - \mathbf{D})}{2} (t_f - t)^2 - \frac{(\dot{\mathbf{T}} - \dot{\mathbf{D}})}{6} (t_f - t)^3 \right] \quad (3.14)$$

We notice that the expression in parentheses in Eq. (3.15) represents the predicted miss distance at time t_f . This gives us a nice insight into the structure of optimal intercept laws and we would expect that the form

$$\mathbf{a}_M = \frac{(t_f - t)}{1/C_1 + \frac{1}{3}(t_f - t)^3} \mathbf{S}(t_f) \quad (3.15)$$

where $\mathbf{S}(t_f)$ is the predicted miss distance at time t_f would hold in general for more complex interceptor and target models, leaving to our ingenuity the method for computing $\mathbf{S}(t_f)$. One may choose C_1 based on engineering judgement or, as in the derivation of proportional navigation laws, we may place more emphasis on minimizing miss distance by letting C_1 go to infinity, obtaining

$$\mathbf{a}_M = 3[\mathbf{S}(t_f)/(t_f - t)^2] \quad (3.16)$$

These last two forms of the optimum guidance laws are ideally suited for application to command guidance instrumentation incorporating a ground computer capable of predicting the final miss distance and time of intercept by using one of the available prediction techniques. For less complicated systems, Eq. (3.14) may be used explicitly, and even if the total acceleration vector of the interceptor is taken as the control vector, the law represents a marked improvement over the usual "proportional navigation" laws because the target acceleration is taken into account. It should be noted that these guidance laws were derived with the implicit assumptions of instantaneous response to commands and the capability of guiding during the total trajectory until intercept. They should be modified, when needed, to incorporate the effects of response delay times and to account for any portions of the trajectory during which no control is available.

References

- 1 Kishi, F. H. and Bettwy, T. S., "Recent Advances in Optimization Techniques," *Proceedings of the Symposium on Recent Advances in Optimization Techniques*, Wiley, New York, 1965.
- 2 Bryson, A. and Ho, Y. C., *Optimization, Estimation, and Control*, Blaisdell Publishing, Waltham, Mass., 1968, Chap. 5.

Similar Solutions for the Laminar Wall Jet in a Decelerating Outer Flow

J. STEINHEUER*

Deutsche Forschungsanstalt für Luft- und Raumfahrt,
Braunschweig, Germany

THE asymptotic behavior for $f''(0) \rightarrow \infty$ of the first new branch of solutions to the Falkner-Skan-equation

$$f''' + f f'' + \beta(1 - f'^2) = 0 \quad (1)$$

with $\beta < 0$, as discovered by Libby and Liu,^{1,2} is discussed and a number of solutions are presented.

The boundary conditions to Eq. (1) are $f(0) = f'(0) = 0$ and $f'(\infty) = 1$; η is the usual similarity variable. The physical interpretation of the new solutions is immediately suggested by the form of the velocity profile $f'(\eta)$ as shown in Fig. 1, i.e., we have a wall jet in a retarded outer flow ($\beta < 0$). It was therefore reasoned that, in the limit, as the overshoot of $f'(\eta)$ becomes increasingly pronounced, the solutions should asymptotically approach the well-known laminar wall-jet solution of Glauert,³ which is a solution to the differential equation

$$F''' + FF'' + 2F'^2 = 0 \quad (2)$$

Equation (2) is identical with Eq. (1) for $\beta = -2$, except for the additive term β in Eq. (1). If, then, the solutions of Eq. (1) for $f''(0) \rightarrow \infty$ are to approach the pure wall-jet solution of Eq. (2), it must be possible to show also that the differential equations assume an identical form for this limiting case. This can indeed be demonstrated by applying the following simple transformation:

$$F(\xi) = A \cdot f(\eta) \quad \eta = A \cdot \xi \quad (3)$$

to the Falkner-Skan equation (1). A is a positive constant. Equation (1) becomes

$$F''' + FF'' + \beta(A^4 - F'^2) = 0 \quad (4)$$

where now the primes denote differentiation with respect to ξ . The previous function $f(\eta)$ and its derivatives are given in terms of the new function $F(\xi)$ as

$$\begin{aligned} f &= (1/A)F & f' &= (1/A^2)F' \\ f'' &= (1/A^3)F'' & f''' &= (1/A^4)F''' \end{aligned}$$

In particular, the relationship between the characteristic values for the wall shear stress is given by $f''(0) = (1/A^3) \cdot F''(0)$. As can be seen, the form of Eq. (4) now becomes identical to the form of Eq. (2) for $A = 0$. On the other hand, the transition process $A \rightarrow 0$ corresponds exactly to the

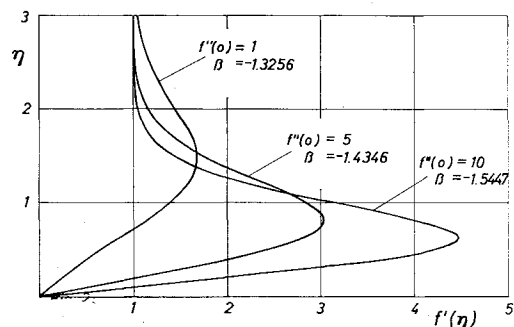


Fig. 1 Typical velocity profiles on the first new branch of solutions to Eq. (1).

Received December 11, 1967.

* Scientific Assistant, Institut für Aerodynamik.

Table 1 Calculated values of β using Eq. (1) with given values of $f''(0)$

$f''(0)$	β	P. A. Libby and T. M. Liu ^a
0	-1.34704	-1.34705
0.005	-1.34704	...
0.01	-1.34703	...
0.015	-1.34702	...
0.02	-1.34695	...
0.05	-1.34679	...
0.08	-1.34652	...
0.1	-1.34627	...
0.15	-1.34547	...
0.2	-1.34443	...
0.3	-1.34182	...
0.4	-1.33883	...
0.5	-1.33578	...
0.8	-1.32822	...
0.9	-1.32665	...
0.95	-1.32606	...
1.0	-1.32562	-1.32563
1.05	-1.32530	-1.32531
1.2	-1.32515	-1.32516
1.5	-1.32792	-1.32793
2.0	-1.33891	-1.33893
2.5	-1.35404	-1.35407
3	-1.37073	-1.37073
4	-1.40399	...
5	-1.43458	...
6	-1.46194	...
7	-1.48622	...
8	-1.50785	...
10	-1.54469	...
15	-1.61156	...
20	-1.65719	...
30	-1.71686	...
40	-1.75510	...
50	-1.78222	...

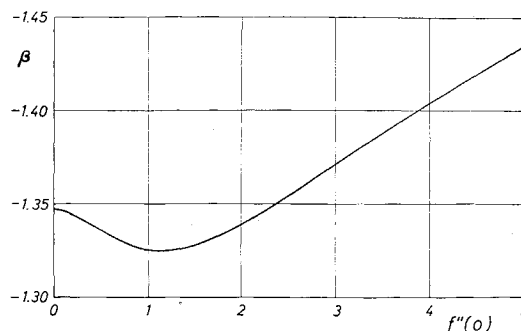
^a By private communication.

limiting process $f''(0) \rightarrow \infty$ if $F'''(0)$ remains finite at the same time.

It remains to be shown that, in the limit $A \rightarrow 0$ [or $f''(0) \rightarrow \infty$], the value of β becomes -2 as in the wall-jet solution. This has been done by numerically computing solutions to Eq. (4). The boundary conditions to Eq. (4) are $F(0) = F'(0) = 0$ and $F'(\infty) = A^2$. In order to apply a simple Runge-Kutta integration scheme in the sense of the "shooting method," the boundary condition at infinity is replaced by the third initial condition $F'''(0) = 1$. Solutions are then sought for a given constant A by varying β in such a way that curve $F'(\xi)$, descending from its maximum, approaches A^2 from above most rapidly. A fast-working iteration scheme was set up for meeting these conditions.

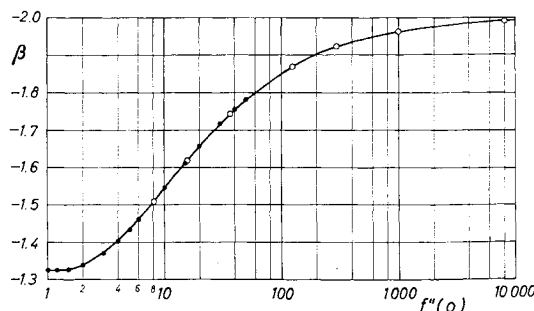
Table 2 Calculated values of β using Eq. (4) with given values of A [$F'''(0) = 1$]

A	β	$f''(0) = 1/A^2$
0.9	-1.32627	1.372
0.8	-1.33764	1.953
0.7	-1.36786	2.916
0.6	-1.42366	4.63
0.5	-1.50787	8.0
0.4	-1.61820	15.62
0.3	-1.74529	37.02
0.2	-1.87013	125.0
0.15	-1.92305	296.3
0.1	-1.96446	1,000
0.05	-1.99090	8,000
0.03	-1.99671	37,020
0.02	-1.99853	125,000
0.01	-1.99963	1,000,000
0	-2 (Glauert)	∞

**Fig. 2** Pressure parameter β vs wall-shear parameter $f''(0)$.

The results of the numerical calculations are displayed in Tables 1 and 2. Table 1 contains β values dependent upon various values of $f''(0) \geq 0$ for solutions of the original Eq. (1). Figure 2 shows a graphical representation of these results. There is a minimum in β at some value of $f''(0)$ near $f''(0) = 1.2$. For comparison, Table 1 contains several values of β as computed by Libby and Liu. There is excellent numerical agreement with the present results. In Table 2, values of β dependent upon the prescribed values of the constant A in Eq. (4) are listed, the third column containing the corresponding values of $f''(0) = 1/A^2$. It can be clearly seen that, as A is chosen closer and closer to zero, β goes to -2 , while $f''(0)$ increases very rapidly towards infinity. This result is displayed in Fig. 3 where a semilogarithmic presentation is used in order to be able to show the dependence of β on the high $f''(0)$ values. The black points correspond to solutions obtained from solving Eq. (1) directly, whereas the circles indicate those solutions which were obtained by solving the transformed Eq. (4). There is exact agreement in the overlapping region, as can also be checked by comparing the values of β for $f''(0) = 8$ and $A = 0.5$ from Tables 1 and 2.

In addition, the solution with the lowest value of A chosen, namely $A = 0.01$ corresponding to $\beta = -1.99963$ (see Table 2), has been compared with Glauert's solution,³ which has the following boundary values: $\hat{F}(0) = \hat{F}'(0) = 0$, $\hat{F}''(0) = \frac{2}{9}$ and $\hat{F}(\infty) = 1$, $\hat{F}'(\infty) = 0$, and the velocity maximum is $\hat{F}'_{\max} = 2^{-5/3} = 0.315$. This solution is easily transformed by the transformation equations (3) to one with the initial conditions $F(0) = F'(0) = 0$ and $F'''(0) = 1$, as were chosen for solving Eq. (4). $\hat{F}(\infty) = 1$ then transforms to $F(\infty) = (\frac{9}{2})^{1/3} = 1.651$, and \hat{F}'_{\max} becomes $F'_{\max} = (\frac{9}{2})^{2/3}$. $\hat{F}'_{\max} = 0.8584$. The corresponding numerical values of the computed solution of Eq. (4) with $A = 0.01$ and $\beta = -1.99963$ are $F(\xi=15) = 1.652$ and $F'_{\max} = 0.8580$. This numerical agreement between a "near" wall-jet solution with the "pure" wall-jet solution is considered a proof for the correct asymptotic behavior of the solutions of Eq. (4) as A tends to zero.

**Fig. 3** Pressure parameter β vs wall-shear parameter $f''(0)$. The curve approaches $\beta = -2$ for $f''(0) \rightarrow \infty$ (see Table 2).

References

¹ Libby, P. A. and Liu, T. M., "Further Solutions of the Falkner-Skan Equation," *AIAA Journal*, Vol. 5, No. 5, May 1967, pp. 1040-1042.

² Libby, P. A. and Liu, T. M., "Some Similar Laminar Flows Obtained by Quasilinearization," *AGARD Seminar on Numerical Methods for Viscous Flows*, Sept. 18-21, 1967, Teddington, England.

³ Glauert, M. B., "The Wall Jet," *Journal of Fluid Mechanics*, Vol. 1, Pt. 6, Dec. 1956, pp. 625-643.

Stresses in a Long, High Mass Fraction Solid-Propellant Rocket Motor

W. G. KNAUSS* AND W. HUFFERD†

Lockheed Propulsion Company, Redlands, Calif.

THE following problem arose in the failure analysis¹ of a solid-propellant rocket motor subjected to slow, uniform cooling. The motor has been idealized by a long quasi-elastic propellant cylinder bonded to the relatively rigid steel case along strips spaced equally around the circumference, the fraction of the perimeter bonded being ρ . Apart from its immediately practical aspect, the problem solution should be of interest in fracture mechanics since the areas of unbondedness correspond to cracks at the interface. The solution can thus provide information on the interaction of N cracks of arbitrarily small size, located on a circle. For $N = 2$ the problem has relevance to that of a disc under diametral compression under two nonslipping curved, rigid punches.

Within the framework of linear elasticity the problem can be formulated as a (plane strain) mixed boundary-value problem such that the displacements are prescribed (const) on part of the perimeter and the tractions vanish on the remainder. Let the uniform temperature change be ΔT , and the difference of the linear coefficient of thermal expansion for the case and the cylinder be $\Delta\alpha$. Then, the constant, prescribed radial displacement on the boundary is $u_0 = (1 + \nu)\Delta\alpha\Delta T$, and the boundary conditions are at $r = 1$

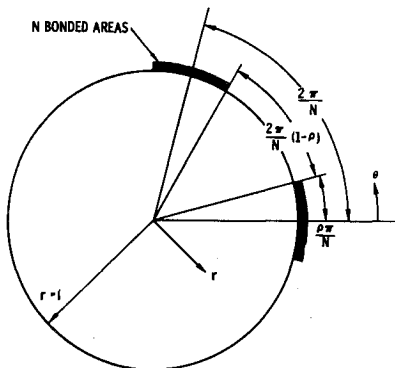


Fig. 1 Two-dimensional geometry of partially bonded, 100% web fraction, solid-propellant grain.

Part of a paper presented at the ICRPG/AIAA Solid Propulsion Conference, Washington, D.C., July 19-21, 1966 (no paper number; published in bound volume of conference papers); received June 17, 1968.

* Consultant; also, Assistant Professor of Aeronautics, California Institute of Technology, Pasadena, Calif. Associate Member AIAA.

† Presently Graduate Student, Division of Engineering, University of Utah, Salt Lake City, Utah. Associate Member AIAA.

(cf. Fig. 1)

$$u_r(1, \theta) = u_0 \quad u_t(1, \theta) = 0$$

$$[2(n-1) - \rho](\pi/N) \leq \theta \leq [2(n-1) + \rho](\pi/N)$$

$$\sigma_r(1, \theta) = \tau_{r\theta}(1, \theta) = 0 \quad (1)$$

$$[2(n+1) + \rho](\pi/N) \leq \theta \leq [2(n+2) - \rho](\pi/N) \quad 1 \leq n \leq N$$

where u_r and u_θ are the radial and tangential displacements and σ_r and $\tau_{r\theta}$ are the corresponding stresses.

Within the concept of the Kolosov-Muskhelishvili² formulation, the problem of finding the stresses and displacements can be reduced to the Hilbert problem of determining a single-valued function ϕ of a complex variable z which satisfies the equations

$$\kappa\phi^+(t) + \phi^-(t) = 2\mu u_0 \quad (2a)$$

on the bonded arcs, where the radial and tangential displacements are prescribed and

$$\phi^+(t) + \phi^-(t) = 0 \quad (2b)$$

on the unbonded arcs where the stresses are prescribed to be zero; μ = shear modulus, $\kappa = 3 - 4\nu$, and ν = Poisson's ratio. Here, t is the value of the complex variable z on the boundary $r = 1$, and the superscript plus and minus signs denote the limits of the function ϕ as the variable t is approached from the inside or outside of the circle $r = 1$. The stresses are derived from ϕ by the relations

$$\sigma_r + i\tau_{r\theta} = \phi(z) - \phi(1/z) + \bar{z}^2[1 - (1/z\bar{z})]\bar{\Psi}(z) \quad (3)$$

$$\sigma_r + \sigma_\theta = 2[\phi(z) + \bar{\phi}(z)] \quad (4)$$

with

$$\bar{z}^2\bar{\Psi}(z) = \bar{\phi}(z) + \phi(1/z) - \bar{z}d\bar{\phi}(z)/dz \quad (5)$$

provided $\phi(z)$ satisfies certain boundedness requirements for $z = 0$ and $z \rightarrow \infty$. Here we have adopted the notation of Ref. 2 with respect to the complex conjugate operations.

Let the end points of the bonded arcs be defined by affixes of the complex numbers (cf. Fig. 1),

$$a_n = \exp\{i[2(n-1) - \rho]\pi/N\} \quad (6)$$

$$b_n = \exp\{i[2(n-1) + \rho]\pi/N\}$$

and let $\beta = (1/2\pi)\log\kappa$. Then, the function

$$\phi(z) = \frac{2\mu u_0}{1 + \kappa} \left\{ 1 + \left[\sum_{n=1}^N C_n z^n \right] \times \left[\prod_{n=1}^N (z - a_n)^{-1/2 - i\beta} (z - b_n)^{-1/2 + i\beta} \right] \right\} \quad (7)$$

made single valued by choosing the branch

$$\phi(z) = [(2\mu u_0)/(1 + \kappa)] \{1 + C_N\} \quad \text{as } |z| \rightarrow \infty \quad (8)$$

can be shown to satisfy Eqs. (2a) and (2b) and, thereby, the boundary conditions on the stresses. It is only necessary to choose the constants C_n so that the displacements u_r and u_θ are also single-valued functions of z , and the stresses are bounded at $r = 0$. This requirement is met if the displacements are continuous and there is no relative displacement between end points of the bonded arcs, which condition is satisfied if the following equations hold:

$$\int_{b_n}^{a_{n+1}} \phi(z) dz = \frac{2\mu u_0}{1 + \kappa} [a_{n+1} - b_n] \quad 1 \leq n \leq N \quad (9)$$

The path of integration may be taken along the traction-free